IJST EXPLORE International Journal of Science and Technology
CENTRE OF PROFESSIONAL RESEARCH PUBLICATIONS
ISSN 2049-7318

International Journal of Science and Technology Volume 2 No. 1, January, 2013

An Investigation on the Effect of Cement Kiln Dust and Glauconite on the Properties of Acid Resisting Brick

Medhat S. El-Mahllawy
Raw Building Materials and Processing Technology Research Institute,
Housing and Building National Research Center (HBRC)
87 El-Tahreer St., Dokki, Giza, Egypt., P.O. Box 1770 Cairo.

ABSTRACT

Cement industry and excavation in iron ore mines in Egypt produced large amounts of cement kiln dust (CKD) and green glauconite in the form of powder and rock fragments, respectively, and have to be discarded. The present work aims to study the effect of cement kiln dust (industrial waste) and glauconite (unexploited quarry material) addition on the properties of acid resisting brick (ARB). This could be cost effective by utilization of these materials in a useful application and it can helpful in tempering the environmental problems associated with such wastes. Three mixtures were designated for studying including variable percentages of clays, CKD, glauconite and Na_2CO_3. Clay based mixtures containing up to 25wt.% glauconite and up to 15wt.% CKD were uniaxially pressed in 5cm side length cube at 22MPa and sintered in an electric furnace (1100-1150^{o}C, for 2h). Results of the physical, chemical and mechanical properties of the made briquettes were assesses according to the Egyptian Standard Specification (ESS) 41-2005. Also, the development of phases and microstructures of selected fired briquettes were characterized using X-ray diffraction (XRD) and scanning electron microscopy (SEM) as well as energy dispersive X-ray (EDX) analysis. The experimental results revealed that the technological properties were found to be strongly influenced by the addition of CKD, glauconite and firing temperature. Also, it was found that decreasing the content of the CKD and increasing of glauconite provided capable vitrified ARB at reasonable sintering temperature. It was confirmed by the recommended briquettes of the mixture M1 (35% kaolin, 35% clay, 5% CKD and 25% glauconite) fired at 1150^{o}C which meets the acid resisting properties according to the ESS at accelerated sintering process, resulting great contributions to economy and ecology of Egypt.

Keywords: *Cement kiln dust, glauconite, acid resisting brick, sintering temperature.*

1. INTRODUCTION

Nowadays, the technological development and the increasing rate at which raw materials are continuously transformed into industrial products result in environmental aggressions and waste generation affecting public health. The use of waste materials as additives in the manufacture of masonry units has been attracting a growing interest of researchers in recent years and is becoming a common practice. With increasing demands of the construction industry, bricks quality and cost become more important day by day in Egypt.

In Egypt, every year huge growing amounts of cement kiln dust (CKD) as a by-product is produced from cement industry during the manufacture of cement clinker by the dry process. The production of different types of cement reached nearly 30 million tons, with at least 3 millions tons CKD/year (Abd El-Aleem et al., 2005). CKD is generally grayish in color and consists predominately of silt-sized, non-plastic particles representing a mixture of partially calcined and unreacted raw feed, clinker dust and fuel ash enriched with alkali sulfates and halides and other volatiles. It is generated as a solid waste from the pre-heater by-pass systems during the manufacture of Portland cement clinker. The properties of CKD depend on the kind of raw materials and the fuel used. The technico-economical-environmental problems arise in the transportation of the dust from the plant to outside as well as the severe pollution to the surrounding environment. As indicated from the literature review that the most common applications for the CKD are in soil stabilization (Peethamparan et al., 2009), hazard mineral removing (Ali et al., 2011; Salem et al., 2012), blended cements (Heikal et al., 2002; El-Mahllawy 2008; Abdel Rahman et al., 2011), manufacturing of vitrified sewer pipes (El Sherbiny et al., 2004), pavement works (Chen and Lin, 2009), ceramic mixtures (Youssef et al., 2004), cement products (Maslehuddin et al., 2008), manufacturing in acid resistant masonry units (El-Mahllawy and El-Sokkary, 2006) and waste water treatment (Waly et al., 2010).

On the other hand, Bahria Oasis mines, Western Desert of Egypt, are the main source of iron ore for the steel industry. The expected reserves of iron ore deposits are about 270 million metric tones (Said, 1990). Iron is presently exploited from El-Gedida area (northeastern plateau of the Oasis). The El-Gedida mine area (Fig.1) is an oval shaped depression up to 15km^2, situated within

the degraded karst cone hills of the Naqb Formation of Middle Eocene age (Hassan and Baioumy, 2007). During the excavation process glauconite beds (as unconformity surface) is appeared overlying the iron ore and must be removed for work progressing. The glauconite is accumulated outside the quarried area as useless friable piles (Fig.2). Thickness of the overlying glauconitic sediments varies from up to 25m in the western and eastern wadi areas to less than 1m in the high central area (Baioumy and Hassan, 2004). Moreover, very little researches have been published on the utilization of the wastes in the manufacture of acid resisting brick. This type of bricks is used as a structural masonry for civil construction that needs high resistance to chemical actions, particularly sewage waters.

The present paper aims to study the effect of addition of cement kiln dust and glauconite on the properties of acid resisting brick in clay based mixtures for economical and environmental benefits. To achieve the aim, physical, chemical and mechanical tests were conducted and assessed according to the ESS 41-2005 in this investigation.

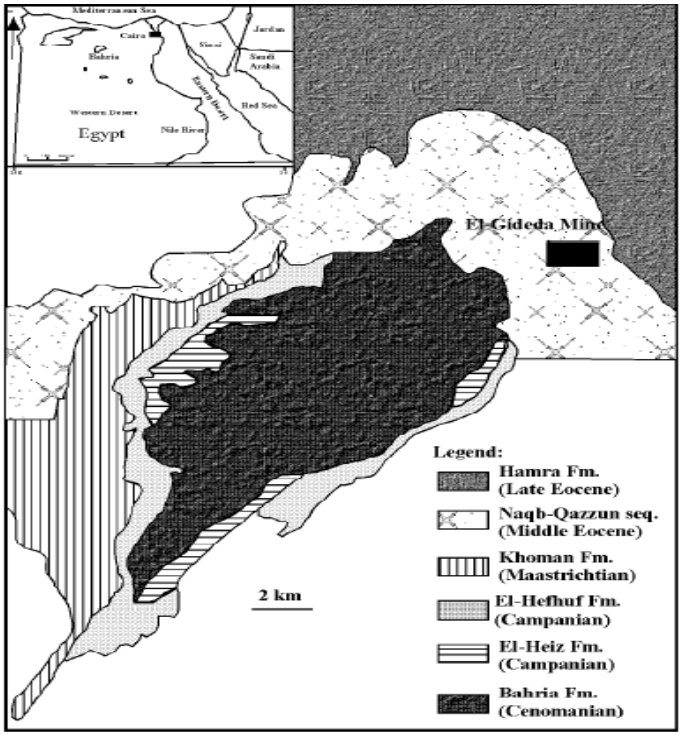

Fig. 1 :Geological map shows the location of El-Gideda iron ore mine, Bahria Oasis, Western Desert, Egypt.

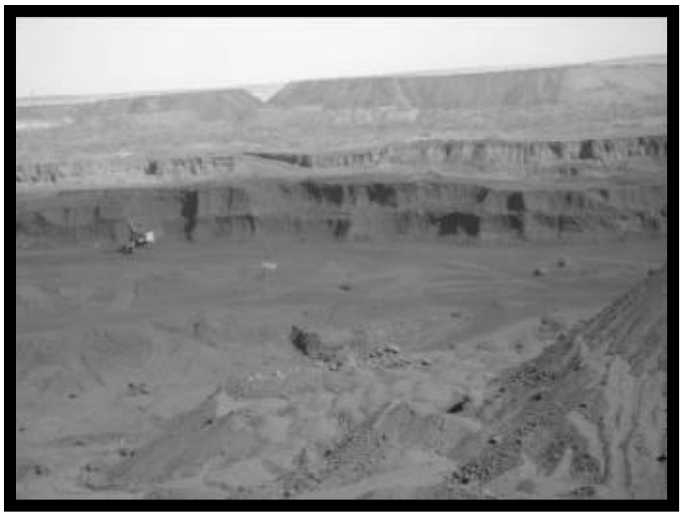

Fig. 2: A field photograph shows locations of the red iron ore (1), green glauconite bed (2) and stockpiles of glauconite (3), El-Gideda iron ore mine site, Bahria Oasis area, Western Desert, Egypt.

2. MATERIALS AND METHODS

In this study, the used starting materials were kaolin, clay, cement kiln dust (CKD), glauconite (Glu) and soda ash. The kaolin material was provided from Tiba Land for Mining Company (Egypt). The clay was collected from a clay quarry located in El-Wadi El-Gedid area, Western Desert. Egypt. The CKD was supplied from Suez Cement Company, Suez, Egypt.

The glauconite was collected from the discarded stockpiles in El-Gideda iron ore site, Bahria Oasis, Western Desert, Egypt. It is located about 270km SW of Cairo and 180km west of the Nile Valley. It was found as dark green rounded pellets with the dimension of a sand grain size. The soda ash (sodium carbonate) was obtained from Alexandria Sodium Carbonate Company, Alexandria, Egypt. It was white powder industrial grade of 99.2% purity.

The used raw materials were characterized by powder X-ray diffraction (XRD). The used XRD apparatus was a X'Pert PRO PW3040/60 (PANalytical) diffractometer equipped with monochromatic Cu-Kα radiation source. The test was run at 40 kV and 30 mA. A continuous mode was used for collecting data in the 2θ range from 5^o to 50^o at a scanning speed 2^o/min. The acquired data were analyzed using X'Pert high score software works with a PDF-2 database. Quantification as a semi-qualitative percentage of the phases was carried out by the X'Pert pro software. The chemical composition (major oxides) of the raw materials was determined by X-ray fluorescence (XRF). The used XRF was an Axios sequential spectrometer manufactured by PANalytical, Netherlands. Also, traditional manual methods prescribed in the American Society for Testing and Materials (ASTM) for determination of the loss on ignition, (LOI), D7348-2008 and insoluble residue (C114-2009) were followed. The methods described in the ASTM (C114-2009) were used for the determination of soluble cations and anions (Na^+, K^+, Cl^- and SO_4^{2-}). Color of the fired briquettes was determined using Munsell's geological rock-color chart.

The microstructure and morphological analyses for selected fired specimens were investigated through the scanning electron microscopy (Leica Steroscan 440, UK). The applied magnification power was up to 3000x with accelerating voltage of 20 kV. The obtained results were analyzed and normalized using energy dispersive X-ray (EDX) attached unit, which helped also in phase identification precisely.

2.1 Mixture Design and Specimen Processing

In order to investigate the feasibility of manufacturing the acid resisting brick (ARB) from the raw materials, three suggested mixtures, namely M1, M2 & M3, were designed for the study. These mixtures composed of constant percentages of kaolin (30wt.%), plastic clay (30wt.%), soda ash (10wt.%) and variable percentages of the CKD (5, 10 and 15wt%) in gradual replacement of glauconite (25, 20 and 15wt.%) as given in Table 1.

Table 1: The mixture composition of the investigated briquettes, wt. %

Symbol	Mixture				
	Clay (Cl)	Kaolin (Ka)	Glauconite (Glu)	Cement kiln dust (CKD)	Soda ash (SA)
M1	30	30	25	5	10
M2	30	30	20	10	10
M3	30	30	15	15	10

It is worthy to record here that from the preliminary experimental tests, it was discovered that the suggested mixtures couldn't achieve the recommended Egyptian requirements without supplementary source acts as inexpensive fluxing agent. The soda ash agent was chosen for this purpose. The used raw materials were crushed, separately dry ground in a laboratory ball

Every mixture was first homogenized in a laboratory blender for 3min.The moisture content (moisture mass / dry mass) was adjusted to 10% before molding. The prepared mixtures were pressed in 5cm-side length cube under a load of 225 kg/cm^2. After forming, the resulting briquettes were dried out in an electrical dryer at 80^oC for 24h, and then fired at different firing temperatures (Tf) of 1100^o, 1125^o and 1150^oC at 5^oC/min firing rate for 2h as a holding time in a controlled laboratory muffle furnace. After finishing the firing program, the specimens were cooled inside the furnace until room temperature. The firing cycle used in the research is shorter than the industrial one providing economical advantage. The mineralogical analysis of the fired test bodies was carried out by the XRD. In order to asses the water absorption, weight loss by acid attack and compressive strength, three fired samples from each mixture were examined against the requirements of the Egyptian standard specification

(41-2005). In addition, volumetric changes and bulk density were calculated. The volume changes were determined using the relation (Vd-Vf)/(Vd), where Vd is the specimen volume before firing and Vf is the specimen volume after firing at a temperature Tf. The bulk density of the fired specimens is determined by dividing the volume over mass of fired briquettes.

3. RESULTS AND DISCUSSION

3.1 Characteristics of the Raw Materials

Table (2) shows the mixture ratios and their calculated chemical composition on calcined basis. The calculated chemical composition of mixtures M1, M2 and M3 exhibited that the most effective fluxing oxides (K_2O, Na_2O and Fe_2O_3) are 21.64%, 20.6% and 19.41% (in descending order), respectively. Due to relatively high amount of the fluxing oxides in the mixture M1 (21.64%) which favour the formation of a considerable vitreous phase, it is expected to form a more abundant glassy phase or its formation at a relatively lower temperature. Also, it is evident from the chemical results of the calculated compositions from the mixtures M1 to M3 that the SiO_2 is decreased with a simultaneous increasing of CaO with the increase of CKD content. In the same way, Fe_2O_3 is increased with the increase of glauconite. The obtained results are agreed with the chemical composition of the starting materials individually (Table 2). Iron oxide is an auxiliary fluxing agent and is responsible for the red color of sintered products (Souza et al., 2010). The glauconite is rich in alkaline flux (K_2O, 6.09%), which tends to accelerate the sintering process.

The raw materials used to prepare acid resisting specimens play an important role in the processing and technological properties. The chemical composition, loss on ignition (LOI) and insoluble residue, if determined, of the materials used is depicted in Table 3. The clay and kaolin demonstrate the expected compositions of SiO_2, Al_2O_3 and Fe_2O_3 that correspond totally to about 77% and 85%, respectively. The glauconite is rich in silica followed by iron and potassium with minor content of other oxides. The high content of iron oxide (21.29%) acts as a flux promoting the liquid phase formation in the sintered body. This result is approved with Christogerou et al., 2009. The CKD is constituted mainly by CaO then SiO_2, accompanied by significant anions content of chloride and sulfate (about 11%). The present content of calcium oxide and anions are reflected on the high content of LOI value (19.59%) and will be responsible for the light coloring of the sintered specimens. The K_2O, Na_2O, Fe_2O_3, CaO, and MgO are considered fluxes and can influence the densification behavior of the ceramic building materials during firing (Segadaes, 2006). From the field observations for the studied Egyptian glauconite (rounded dark green pellets of sand grain size) and the insoluble residue result (42%) consequently it can be called as green sand especially after the coloration by green color caused by glauconite.

Table 2: The mixture ratios included 10% Na_2CO_3 and their calculated chemical composition on calcined basis

Mixture	Mixture composition, wt. %				Chemical composition, wt. %									
	Cl	Ka	Glu	CKD	SiO_2	Al_2O_3	Fe_2O_3	CaO	MgO	Na_2O	K_2O	SO_3	TiO_2	P_2O_5
M1	30	30	5	25	54.49	16.13	9.27	5.01	1.91	7.01	2.72	0.72	1.28	1.43
M2	30	30	10	20	52.63	16.11	8.23	8.08	1.74	7.22	2.59	0.74	1.29	1.28
M3	30	30	15	15	50.73	16.08	7.17	11.21	1.57	7.45	2.45	0.77	1.30	1.12

Table 3: Chemical composition in terms of oxide content, soluble anions, insoluble residue and loss on ignition of the raw materials on dry basis, wt. %

Oxide content %	Clay	Kaolin	Glauconite	Cement kiln dust

SiO_2	60.14	53.67	49.18	8.29
Al_2O_3	9.69	31.04	5.98	2.84
Fe_2O_3	7.63	0.84	21.29	2.07
CaO	5.15	0.16	0.48	51.90
MgO	2.11	0.12	3.77	0.57
Na_2O	5.76	0.02	0.11	2.63
K_2O	0.88	0.04	6.09	3.42
SO_3	0.15	0.03	1.85	2.09
*TiO_2	1.24	2.24	2.20	0.14
Cl^-	ND			6.12
SO_4^{2-}	ND			4.80
Insoluble residue	ND		42.0	ND
L.O.I	6.28	12.63	8.07	19.59

The powder XRD patterns for the starting raw materials of kaolin, clay, glauconite and CKD are manifested in Fig. 3. The minerals identified for kaolin are kaolinite [$Al_2Si_2O_5(OH)_4$] and quartz [SiO_2]. The clay sample is composed of montmorillonite [$Na,Ca)_{0.33}(Al,Mg)_2(Si_4O_{10})(OH)_2 \cdot nH_2O$], kaolinite and quartz minerals. The crystalline minerals in the glauconite sample is constituted from glauconite [$(K,Na)(Fe^{3+},Al,Mg)_2(Si,Al)_4O_{10}(OH)_2$], kaolinite and muscovite [$KAl_2(Si_3Al)O_{10}(OH,F)_2$]. The CKD pattern shows that lime [CaO] is the major crystalline phase whereas portlandite [$Ca(OH)_2$], quartz, sylvite [KCl], calcite [$CaCO_3$] and larnite [Ca_2SiO_4] are minor phases.

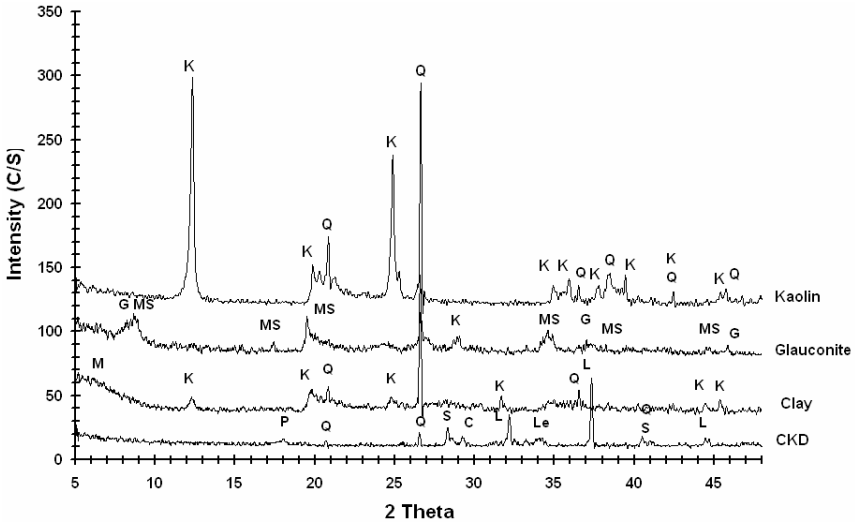

Fig. 3: X-ray diffraction patterns of the used materials (K: Kaolinite, Q: Quartz, G: Glauconite, Mi: Mica, MS: Muscovite, M: Montmorillonite, P:Portlandite, S: Sylvite, C: Calcite, Le: Larnite, L: Lime).

3.2 Mineralogy of the Fired Briquettes

Figs. 4-6 demonstrate the XRD patterns of the briquettes that made from different mixtures (M1-M3) as function with firing temperatures. The data enclosed in Table 4 shows a summary for the phases composition (%) identified in the XRD patterns of the fired briquettes. From these results it was found that the crystalline phases in all mixtures are quartz [SiO_2], anorthite [$CaAl_2Si_2O_8$], augite [$(Ca,Na)(Mg,Fe,Al,Ti)(Si,Al)_2O_6$] and albite [$NaAlSi_3O_8$] with variable percentages. Also, it was noticed that anorthite and albite are the main phases in all fired mixtures whereas augite is beginning to develop. Also, augite is completely disappeared in the mixture M3 at all firing temperatures at the expense of formation of anorthite and albite phases. During the firing series of reactions and transformations take place in the briquettes between minerals, which will be decisive in establishing the final properties of the fired product. It can be observed that the quartz peak increases in intensity till 1125^{o}C then decreases slightly due to its partial dissolution forming amorphous silica and the viscous liquid phase converted to glass after cooling (Souza et al., 2010). According to Souza et al., 2010, the reactions and transformations that

may take places are: (1) between ~450 – 600°C, kaolinite loses the OH groups of the gibbsite layer leading to formation of amorphous metakaolinite, (2) at ~950 – 1000°C, the silicate lattice of clay material is totally collapsed, followed by reorganization of the metakaolinite structure and the formation of amorphous silica. It is worthy to note that the CaO of CKD reacts during firing with the quartz and metakaoline and metastable wollastonite and gehlenite are expected to appear but due to increasing the temperature the augite is formed instead on. This result is concordant with Montero et al., 2009. Also, the formation of crystalline phase of anorthite is predictable to occur at a great extent at the expense of the metakaolin (Kurama et al., 2007). In addition to, structural transformation of metakaolinite to gehlenite is well known. The last phase is unstable (intermediate phase) and formed from the reaction between metakaolinite and calcium oxide. Later anorthite is formed from gehlenite, which is combined with silica and alumina rich phase (Baccour et al., 2008).

Apart of SiO_2 did not react because its quantity was in excess of free silica. So, it is found in all the XRD patterns. In view of high firing temperatures normally used, the vitrified products have a high glassy phases content which improves chemical resistance against leaching (Montero et al., 2009).

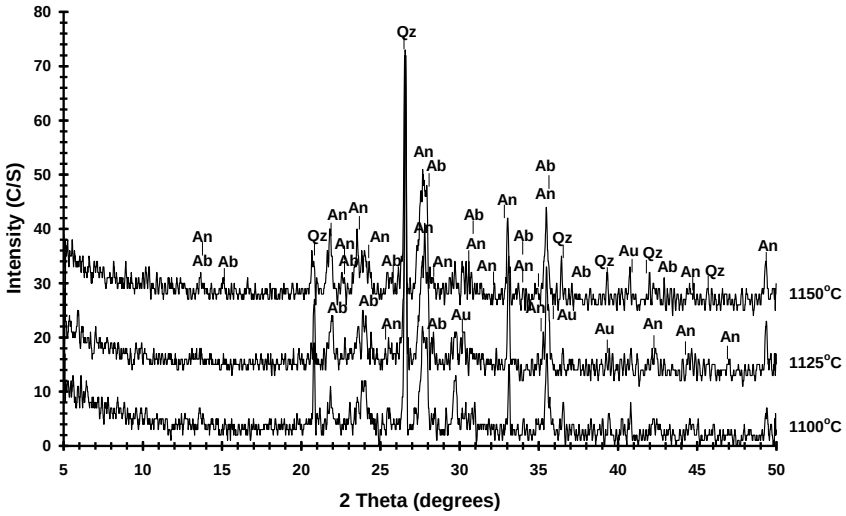

Fig. 4: X-ray diffraction patterns of specimens of the mixture M1 fired at different firing temperatures (A: Anorthite, Q: Quartz, Ab: Albite, Au: Augite).

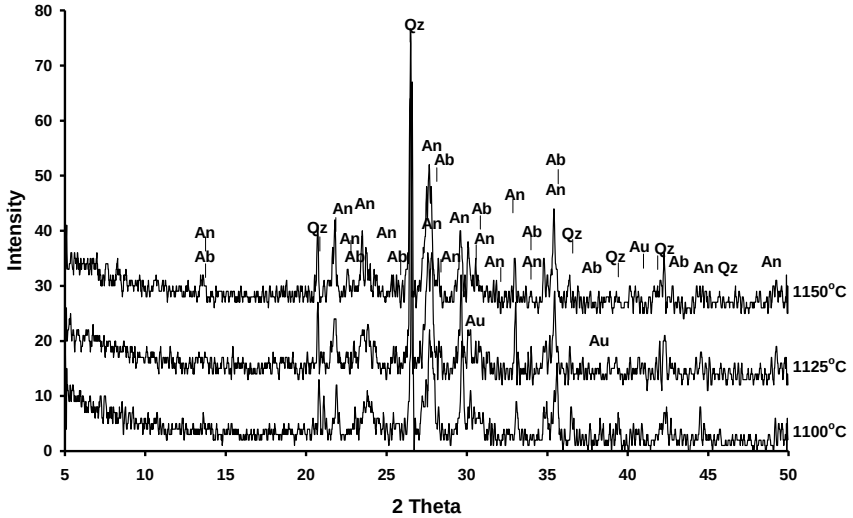

Fig. 5: X-ray diffraction patterns of specimens of the mixture M2 fired at different firing temperature A: Anorthite, Q: Quartz, Ab: Albite, Au: Augite).

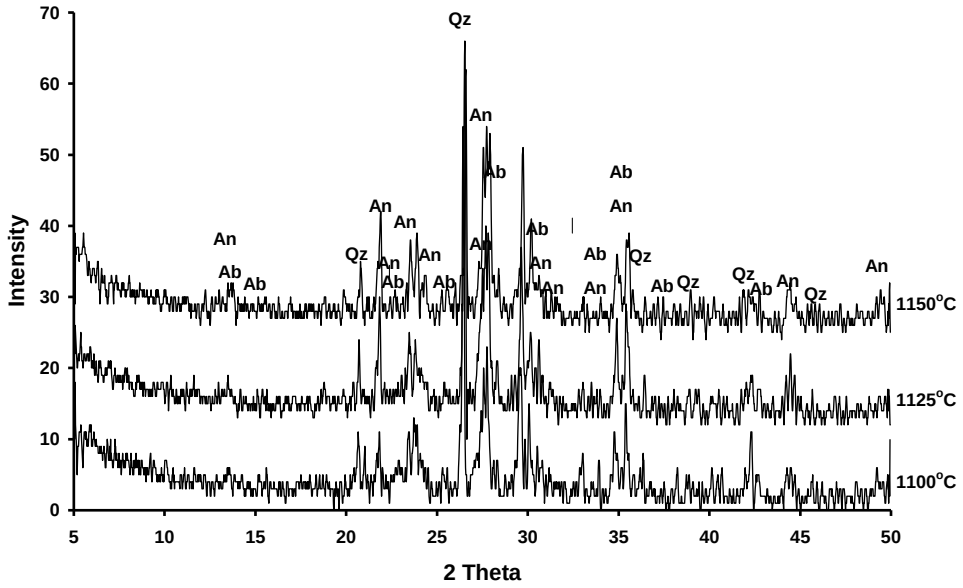

Fig. 6 :X-ray diffraction patterns of specimens of the mixture M3 fired at different firing temperatures (A: Anorthite, Q: Quartz, Ab: Albite, Au: Augite).

Table 4: Phase developed (%) by the XRD for the fired briquettes of different mixtures

Mixture / firing temperature, °C	Phase developed				CKD : Glu ratio
	Quartz	Anorthite	Augite	Albite	
M1					5 : 25
1100	17	27	10	46	
1125	20	38	13	29	
1150	9	40	-	51	
M2					10 : 20
1100	19	36	19	26	
1125	22	-	15	63	
1150	7	-	13	80	
M3					15 : 15
1100	12	35	-	53	
1125	17	55	-	28	
1150	5	68	-	27	

The anorthite phase increased by increasing the firing temperature as well as the CKD content as found in the mixture M3(CKD: 15% and CaO: 11.21%). Similar phase was reported in the literature for clay materials with high calcium oxide content (Baccour et al., 2008). The formation of anorthite may be due to interaction between the silica of glauconite, aluminum of clays and calcium of CKD to form calcium aluminum silicate phase. It is evident from tables 3 and 4 that in the mixture M3 (the highest content of CKD, 15%, and lowest content of glauconite, 15%) the silicon oxide and iron oxide are decreased and calcium oxide is increased giving an opportunity to the formation of quartz, anorthite and albite phases at the expense of augite formation. Consequently, the augite phase does not appear in mixture M3 at all firing temperatures. This disappearing is simultaneous associated with the increase of anorthite phase. On the other hand, it is needless to say that the CKD is a product from a high temperature process, so it is inert to sintering process if the temperature is not high enough. In addition to, the decrease of quartz phase with the increase of firing temperature can be attributed to that the quartz mineral is completely developed at 1125°C and then begin to dissolute in the liquid phase formed from the impurities (Na_2O, K_2O, Fe_2O_3 and CaO) present in the mixture composition (Baldo and dos Santos, 2002) as well as its sharing in anorthite formation which already increases with the increase of firing temperature. The presence of

anorthite in the XRD patterns reveals that the firing process is reached to the equilibrium state giving evidences that reaction is completed (El-Mahllawy, 2008). As regards the mineralogical analysis, there are no new phases formed after 1100°C with different mixtures and firing temperatures, the difference is only in the phase intensity.

3.3 Scanning Electron Microscopy (SEM) Analysis

Scanning Electron Microscopy (SEM) technique with Energy Dispersive X-ray (EDX) analysis was employed to obtain a view of the microstructure and to conduct an analysis on the morphology, surface texture and composition of the fractured surfaces of selected fired briquettes of different mixtures. Figs 7and 8 explain the SEM micrographs and their corresponding EDX elemental oxides.

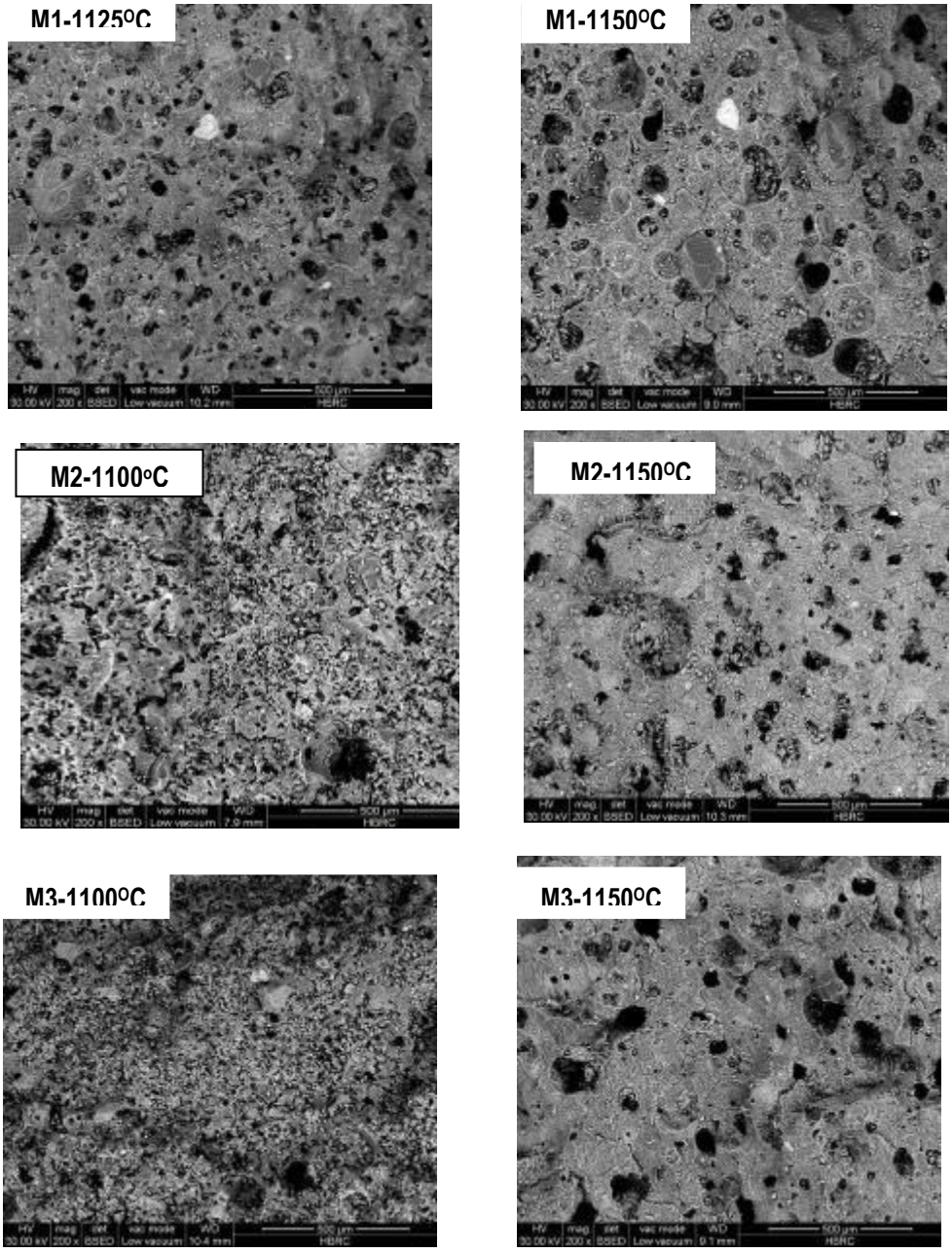

Fig.7: SEM micrographs show effect of the sintering temperature on the microstructure of fired briquettes made from different mixtures, magnification power 200x.

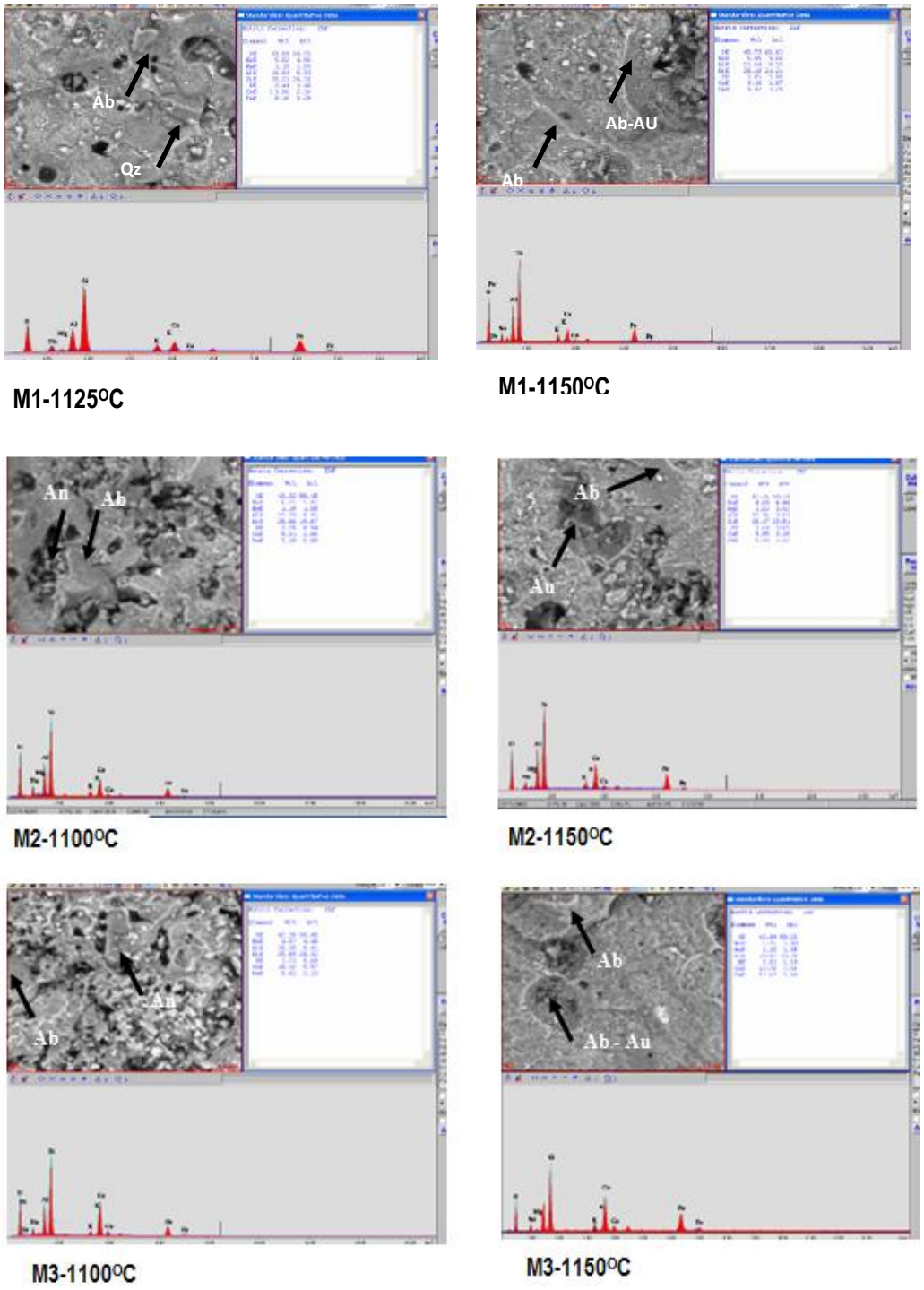

Fig. 8: EDX elemental micrographs of a general view of the fired briquettes of different mixtures, magnification power 1359x (An: Anorthite, Ab: Albite, Au: Augite, Qz: Quartz).

The SEM micrographs show clearly a different degree of densification and a progressing in pore closing by the formed phases with firing temperature and glauconite content affecting constructively on the technological properties of the fired briquettes.

The formed phases appear as intergrowth texture with the development in pore closing, particularly with firing temperature increasing. Also, the SEM images represent nearly disappearing of the well defined crystalline phases in a glassy matrix. Widespread, not interlinked open pores are easily distinguishable in the glassy matrix as dark grey spots. SEM image of the mixture M1 fired at 1150°C show a well compacted and vitrified structure with less open pores more than the other images, M2 and M3. This will provide the fired briquettes with superior properties. As the microstructure becomes more compact (at high temperatures), pores become isolated rather than as channels.

The presence of isolated rounded pores suggests that the material reached the final sintering stage (Souza et al., 2010). Thus, the introduction of glauconite material in the M1 briquette formulation brought positive microstructure, resulting in significantly denser structure. On the contrary, the CKD addition provides less dense structure as appeared in the SEM images of the mixture M3.

Also, the SEM micrograph of the mixture M3 fired at 1150°C exhibits large pore volume and less filled with other phases comparable with the other micrographs, M1 and M2. This indicates a sign that it begins to achieve the sintering temperature. Therefore, high firing temperature (more than 1150°C) or more holding time (more than 2h) may be needed to enhance the structure of specimens of M2 and M3. Although the microstructure of M3 shows open pore to form communicating channels, the structure is compacted and the degree of vitrification is advanced, particularly at 1150°C.

EDX images (Fig. 8) match the mineralogical composition of the XRD analysis. The elemental analysis suggest presence of quartz, albite, anorthite and augite phases with different grain forms and all are found in the glassy matrix.

Albite and quartz crystals are well developed. Results of the SEM and EDX analyses are in agreement and confirmed with those presented in the mineralogical analysis by the XRD analysis.

3.4 Technological Properties of the Fired Briquettes

Average results of physical, chemical and mechanical properties of the fired briquettes formulated from different mixtures are listed in Table 5 and graphically represented in Fig. 9.

- Color of the fired briquettes according to Munsell's color system clarified that the fired briquettes color became darker (very dark red) with both of firing temperature and glauconite content increasing and getting lighter (light brown) with the CKD content. This can be attributed to the increasing of the iron content within the mixture itself with increasing glauconite, which will be responsible for the dark coloring of the sintered bodies. It was confirmed by the iron content (Table 3) in mixture M1 reached 9.27% (very dark red at 1150°C) and in mixture M3 it attained only 7.17% (dark yellowish brown at 1150°C).

Table 5: Results of surface texture and color of the fired briquettes as function of the formulated mixtures and firing temperatures.

Mix code	Surface texture			Color according to Munsell's color chart		
	1100°C	1125°C	1150°C	1100°C	1125°C	1150°C
M1	Rough		Smooth	Moderate Red (5YR 5/6)	Dusky Red (5R 3/4)	Very dark Red (5R 2/6)
M2	Rough			Light brown (5YR 5/6)	Moderate Brown (5YR 4/4)	Grayish red (5R 4/2)
M3	Rough			Light brown (5YR 6/4)	Moderate yellowish Brown (10YR 5/4)	Dark yellowish Brown (10YR 4/2)

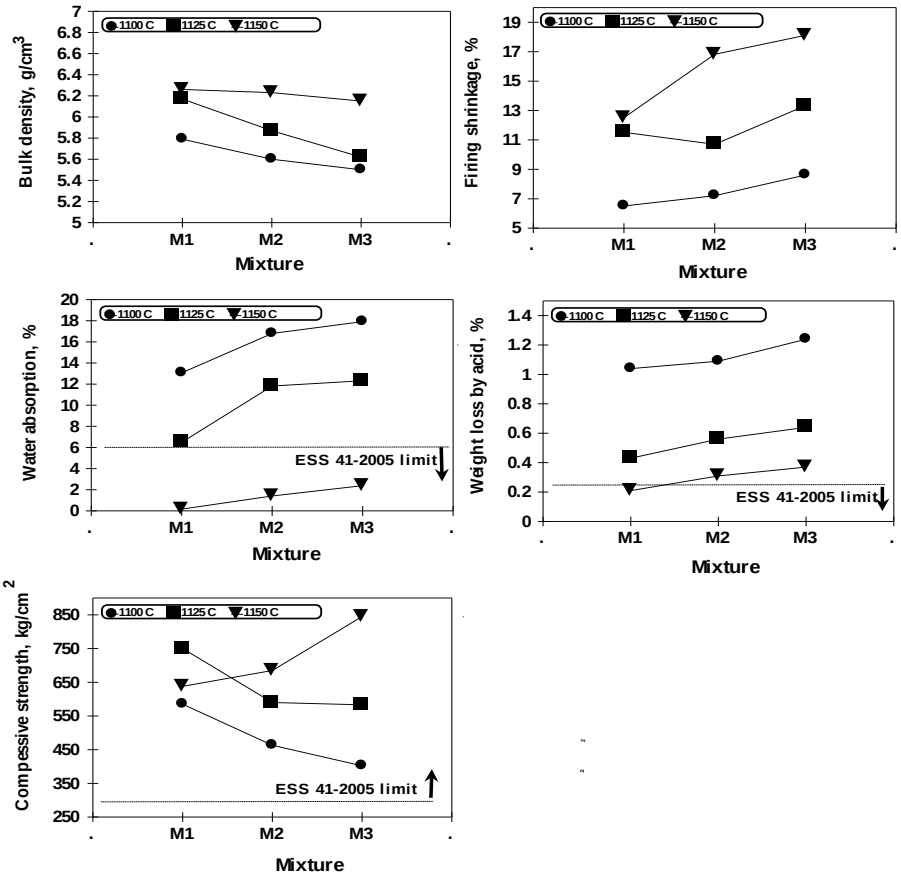

Fig. 9: Variation in the properties of fired briquettes as function of formulated mixtures and firing temperatures.

- Surface texture for all fired briquettes shows a rough touch except for the briquettes of the mixture M1 fired at 1150°C, it shows a smooth surface texture (glazed touch). It implies, further firing temperature for the briquettes of mixture M1 should be avoided due to the expected deformation. This may be due to reaching briquettes of the mixture M1 (5wt.% CKD and 25wt.% glauconite) to the optimum sintering temperature which enhances vitrification. Also, the glazed surface texture may be attributed to the large amount of iron oxide (9.27wt.%) which promotes rapid vitrification and fusion during firing.

- In terms of bulk density of the fired briquettes, it is increased with firing temperature and glauconite content. Briquettes of the mixture M1 demonstrate the highest density (6.26g/cm^3 at 1150°C) and for the mixture M3 it shows the lowest one (6.15g/cm^3 at 1150°C). In other words, as glauconite content increases (M1), at the expense of CKD content, the bulk density increase giving evidence for densification and vitrification improvement. By the action of capillarity and surface tension the particles undergo a rearrangement that promotes densification. On the other hand, the substantial increase in the bulk density with firing temperature is in line with the formation of a more abundant liquid phase during firing that fills the open pores and reduces the open porosity. Also, it can seen from the bulk density graph that the bulk density decrease slightly with the CKD content. This decreasing in bulk density can be regarded as a result of the increase in porosity in the fired bodies either for gas releasing (weight loss) or volume expansion, bloating (Souza et al., 2010).

- Results of the firing volume shrinkage depict a continuous increasing in the shrinkage for all briquettes which increases with both of firing temperature and CKD content. It reached the lowest value (6.51%) for briquettes of mixture M1 at 1100°C and the highest value (18.11%) for briquettes of mixture M3 at 1150°C. The shrinkage increasing with increasing firing temperature is a consequence of vitrification, which occurs during the sintering process helping to reduce porosity if the sintering temperature was enough and extended to a reasonable holding time. Also, briquettes of the mixture M1 achieved the lowest shrinkage values compared with the others briquette mixtures. This behavior can be attributed to the highest amount of sand (quartz) in glauconite (Maximum: 25% in M1 mixture composition) as appeared in the insoluble residue result (42%) which is a non-plastic component.

- The results of water absorption clarify a rapidly decreasing with firing temperature and glauconite content. This is essential due to the high amount of glassy phase formed during firing, which decreases the open porosity

by the filling with the glassy phase causing densification of the ceramic body (Moreira et al., 2008). Also, water absorption increases with the CKD content giving indication to the porosity increasing. This is confirmed with the result of bulk density. Whereas the highest water absorption result is found for the briquettes of the mixture M3 (17.91% at 1100^{o}C) which is corresponded with the lowest bulk density for the briquettes of the same mixture (5.50 g/cm^{3} at 1100^{o}C). It is expected that the liquid phase formed during the sintering is not enough to cause a sharp decrease in porosity (i.e. densification).

According to the studied ESS 41-2005, only the briquettes fired at 1150^{o}C achieved the Egyptian specification for the acid resisting brick (water absorption value < 6%) and can be considered as a well sintered briquettes. This means that the water absorption decreasing is associated with a more significant liquid phase formation. The liquid phase penetrates the open pores closing them and isolating neighboring pores. On the other hand, the decline in water absorption values suggests that the replacement of CKD by glauconite improves densification. This is probably due to the reduction of the viscosity of the glassy phase, which accelerates the sintering process (Segadaes, 2006).

- Results of the weight loss due to acid attack of the fired briquettes show a decreasing with firing temperature and glauconite content. Also, it is indicated that the weight loss is not only has a relationship with firing temperature but also with water absorption property. As the weight loss decrease the water absorption decrease and firing temperature increase. This is presumably due to the decrease of open pores which is supported with the briquettes of mixture M1. It is brought the highest resistance toward acid attack (0.21%) and couple with the lowest water absorption value (0.17%), both properties are a result of vitrification process. According to the studied ESS, only the briquettes of mixture M1 (0.21%) fired at 1150^{o}C achieved the Egyptian specification for the acid resisting brick (weight loss value by acid attack < 0.25%).

- Results of the compressive strength point to that the compressive strength increase with the increase of firing temperature, except for the briquettes of mixture M1, and CKD content. It is decreased after 1125^{o}C. After this temperature the glassy phases are formed vigorously, more than necessary, as seen by the necked eye (glazed surface) and the SEM analysis where the briquettes become breakable. If the glass phase is too much, the bricks will show the character of brittle material to decrease the compressive strength due to gas entrapment (Song et al., 2011). Accordingly, firing of the briquettes (M1) more than 1150^{o}C should be avoided. Firing more than 1150^{o}C, since the vitrification was completed, for the briquettes of mixture M1 is probable cause pores joining together to form large pores causing macroscopic deformation (Baccour et al., 2008). Also, the results show that the briquettes of mixture M3 (15% CKD) have the highest compression value (845kg/cm^{2}) at the firing temperature of 1150^{o}C. This may due to the highest content of the anorthite phase. The better mechanical performance is usually ascribed to the formation of calcium aluminum silicates, such as anorthite, gehlenite or wollastonite phases (Acchar et al., 2006; Taskiran et al., 2005). The briquettes of M3 represent the highest content of anorthite phase which increases with firing temperature (Table 4); 35% at 1100^{o}C and 86% at 1150^{o}C. On the other hand, higher amount of glassy phase will be formed during firing, to a reasonable extent, which decreases the open porosity by the filling with the glassy phase causing densification and strengthen the ceramic body. In spite of the compressive strength results, all the fired briquettes are met the limits of the studied ESS (compressive strength value > 300 kg / cm^{2}).

Based on the obtained results from the technological properties, it is suggested to add more content of the CKD a high temperature (more than 1150^{o}C) is needed to fulfill the studied ESS, particularly water absorption and weight loss by acid attack limits.

It is worth mentioning that the decrease in water absorption values and an increase in volume shrinkage with increasing firing temperatures are due to effective formation of a liquid phase which hinders cracks formation and improves the mechanical strength. This is agreed with Monteiro et al., 2004.

4. VISUAL INSPECTION

The recommended fired acid resisting briquettes (M1, 1150^{o}C) are of solid type and painted with very dark red color. They characterized by a regular shape, straight and flat surfaces. Also, the made briquettes have no cracks, bulges and free from bumps or visible defects.

5. CONCLUSIONS

The characteristics and feasibility of acid resisting brick made of clay based mixtures with the cement kin dust (industrial waste) and glauconite material (unexploited quarry product) were investigated in this research. The results presented along this work enable to draw the following conclusions:

1. Experimental results demonstrate clearly that the briquettes properties are strongly dependent on both of the added materials (CKD and glauconite) and firing temperature.

2. Soda ash material should be added as a supplementary fluxing agent in the studied mixtures.

3. Increasing of CKD in the investigated mixtures should be avoided hence it leads to deleterious in the technological properties of the acid resisting briquettes.

4. Only the fired briquettes formulated from the mixture M1, 5% CKD and 25% glauconite, fired at 1150°C through accelerated sintering process can be utilized for making acid resistance brick.
5. There are no new crystalline phases formed during the sintering process after 1100°C.

6. To achieve briquettes with a high content of the CKD, optimization of the sintering profile or changing the type of fluxing material may be needed.

7. Based on this work an environmentally brick, with good commercial characteristics was made using recycling technology in a safe disposal manner for the studied pollutants.

ACKNOWLEDGEMENTS

The author would like to express his gratitude to Dr. Ayman M. Kandeel, Professor of cement technology, from the HBRC for the help in the experimental work and additional comments. Also, the contribution of Mrs. Duaa M. Hefni is gratefully acknowledged.

REFERENCES

[1] Abdel Rahman, A., S.A. Abo-El-Enein, M. Aboul-Fetouh, and Kh. Shehata, 2011. Characteristics of Portland blast-furnace slag cement containing cement kiln dust and active silica. Arabian Journal of Chemistry, In Press, Corrected Proof Research Article.

[2] Abd El-Aleem, S., M .Abd-El-Aziz, M. Heikal and H. El-Didamony, 2005. Effect of cement kiln dust substitution on chemical and physical properties and compressive strength of Portland and slag cements. The Arabian J. Sci. and Engineering, 30 (2B): 362-273.

[3] Acchar, W., F. A.Vieira and A. M. Segadaes, 2006. Using ornamental stone cutting rejects as raw materials for red clay ceramic products: Properties and microstructure development. Matr. Sci. Engineering, A 435: 606-610.

[4] Ali, O.I., H.H.Osman, S.A. Sayed and M.E.Shalabi, 2011. The removal of some rare earth elements from their aqueous solutions on by-pass cement dust. J. Hazardous Materials, 195: 62-67.

[5] ASTM C114, 2009. Standard test method for chemical analysis of hydraulic cement. Standard Annual Book of ASTM Standards, USA. 04.01.

[6] ASTM D7348, 2008. Standard test methods for loss on ignition (LOI) of solid combustion residues. Standard Annual Book of ASTM Standards, USA. 05.06.

[7] Baccour, J., M. Medhioub, F. Jamoussi and T. Mhiri, 2008. Densification behaviour of a red firing Tunisian Triassic clay. American J. Appl. Science, 5 (3): 263-269.

[8] Baioumy, H. and M. Hassan, 2004. Authigenic halloysite from El-Gideda iron ore, Baharia Oasis, Egypt: characterization and origin. Clay Mineral, 39: 207-17.

[9] Baldo, J. and W.dos Santos, 2002. Phase transition and their effects on the thermal diffusivity behavior of some SiO_2 polymorphs. Ceramica, 48: 307-320.

[10] Chen, L. and D. Lin, 2009. Stabilization treatment of soft subgrade soil by sewage sludge ash and cement. J. Hazardous Materials, 162 (1): 321-327.

[11] Christogerou, A., T. Kavas, Y. Pontikes, S. Koyas, Y. Tabak and G. N. Angelopoulos, 2009. Use of born wastes in the production of heavy clay ceramics. Ceram. International, 35: 447-452.

[12] Egyptian Standard Specification (ESS), 2005. Acid-resisting bricks for lining sewerages tunnels. Egypt. Asso. Qual. Spec. 41: 1-5.

[13] El-Mahllawy, M. S., 2008. Characteristics of acid resisting bricks made from quarry residues and waste steel slag. Construction and Building Materials, 22: 1887-1896.

[14] El-Mahllawy, M. and T.El-Sokkary, 2006. Recycling of cement kiln dust and waterglass sludge in the manufacture of acid resistant masonry units. J. Housing and Building National Research Center (HBRC), 2 (1): 23-35.

[15] El Sherbiny, S.A., N.F.Youssef, O.A. Ibrahim and M.F.Abadir, 2004. Use of cement dust in the manufacture of vitrified sewer pipes. Waste Management, 24 (6): 597-602.

[16] Hassan, M. and H. Baioumy, 2007. Characterization and origin of alunite in the El-Gideda iron mine (Egypt). Periodico di Mineralogia (Per. Mineral.) 76 (1): 11-24.

[17] Heikal, M., I.Aiad and I.M Helmy, 2002. Portland cement clinker, granulated slag and by-pass cement kin dust composites. Cement and Concrete Research, 32 (11): 1805-1812.

[18] Kurama, S., A. Kara and H. Kurama, 2007. Investigation of borax waste behaviour in tile

production. J. Euro. Cream. Society, 27: 1715-1720.

[19] Maslehuddin, M., O. Al-Amoudi, M. Shameem, M. Rehman and M. Ibrahim, 2008. Usage of cement kiln dust in cement products-research review and preliminary investigations. Construction and Building Materials, 22 (12): 2369-2375.

[20] Montero, M.A., M.M. Jordan, M. S. Hernandez-Crespo and T. Sanfeliu, 2009. The use of sewage sludge and marble residues in the manufacture of ceramic tile bodies. Appl. Clay Science, 46: 404-408.

[21] Montero, M.A., M.M. Jordan, M. B. Almendro-Candel, T. Sanfeliu and M. S.Hernandez-Crespo, 2009. The use of a calcium carbonate residue from the stone industry in manufacturing of ceramic tile bodies. Appl. Clay Science, 43: 186-189.

[22] Monteiro, S. N. and C. M. Vieira, 2004. Influence of firing temperature on the ceramic properties of clays from Campos dos Goytacazes, Brazil. Appl. Clay Science, 27: 229-234.

[23] Moreira, J. M., J. P. Manhaes and J. N. Holanda, 2008. Processing of red ceramic using ornamental rock powder waste. J. Matr. Proc. Technology, 196: 88-93.

[24] Peethamparan, S., J. Olek and S. Diamond, 2009. Mechanism of stabilization of Na-montmorillonite clay with cement kiln dust. Cement and Concrete Research, 39 (7): 580-589.

[25] Salem, A., H. Afshin and H. Behsaz, 2012. Removal of lead by using Rasching rings manufactured with mixture of cement kiln dust, zeolite and bentonite. J. Hazardous Materials, In Press, Accepted Manuscript.

[26] Said, R., 1990. The geology of Egypt. Elsevier, New York, 734pp.

[27] Segadaes, A. M., 2006. Use of phase diagrams to guide ceramics production from wastes. Adv. Appl. Ceramics, 105: 46-54.

[28] Souza, A. J., B. C. Pinheiro and J. N. Holanda, 2010. Recycling of gneiss rock waste in the manufacture of vitrified floor tiles. J. Envi. Management, 91: 685-689.

[29] Souza, A. J., B. C. Pinheiro and J. N. Holanda, 2010. Processing of floor tiles bearing ornamental rock-cutting waste. J. Matr. Procs. Technology. 210: 1898-1904.

[30] Song, J., F. Wang, X. Bai, D. Du, Y Ju, M. Xu and G. Ji, 2011. Effect of the sintering technology on the properties of fired brick from quartz sands. J. Ceram. Proc. Research, 12 (4): 357-360.

[31] Taskiran, M., N. Demirkol and A. Capoglu, 2005. A new porcelainised stoneware material based on anorthite. J. European Ceram. Society, 25 (4): 293-300.

[32] Waly, T., A. Dakroury, G. El-Sayed and S. El-Salam, 2010. Assessment removal of heavy metals ions from wastewater by cement kiln dust (CKD). J. American Science, 27: 1715-1720.

[33] Youssef, N., T. El-Sokkary and M. El-Mahllawy, 2004. Simultaneous utilization of cement kiln dust and blast furnace slag in ceramic floor tile mixtures. Int. Conf. Future Vision and Challenges for Urban Development. 209-22 Dec.,Cairo, Egypt, EE11F.